

## Efficiency limits of rectenna solar cells: Theory of broadband photon-assisted tunneling

Saumil Joshi and Garret Moddel<sup>a)</sup>

Department of Electrical, Computer, and Energy Engineering, University of Colorado, Boulder, Colorado 80309-0425, USA

(Received 16 November 2012; accepted 11 February 2013; published online 26 February 2013)

Because rectifiers can convert a wide range of frequencies to dc it was thought that rectenna solar cells—antennas coupled to ultra-high speed diodes—could efficiently harvest the entire solar spectrum and exceed the Shockley-Queisser limit. We show that there are efficiency limits to broadband optical conversion and provide a quantitative analysis using the theory of photon-assisted tunneling. This quantum-based approach differs from classical rectification in lower frequency rectennas. The conversion efficiency approaches 100% for monochromatic illumination. For broadband illumination at terrestrial solar intensities, the diode operating voltage plays the role that bandgap plays in conventional solar cells. © 2013 American Institute of Physics. [<http://dx.doi.org/10.1063/1.4793425>]

Optical rectennas, submicron antenna-coupled high speed diodes, have been proposed for harvesting solar energy as an alternative to conventional semiconductor photovoltaic devices.<sup>1</sup> In contrast to optical rectennas, conventional solar cells have a bandgap that constrains their conversion efficiency to the Shockley-Queisser limit.<sup>2</sup> We examine the response of optical rectennas to broadband blackbody radiation. To explain the operation of optical rectennas under multispectral illumination we use the theory of photon-assisted tunnelling (PAT).<sup>3</sup>

PAT theory and experiments have been investigated for superconducting junctions used as photon detectors.<sup>4,5</sup> For these devices, semi-classical (quantum) behavior comes into play when the photon energy divided by the electron charge ( $\hbar\omega/q$ ) becomes large compared to the voltage at which significant nonlinearity appears in the diode current-voltage [ $I(V)$ ] characteristics.<sup>6</sup> We apply PAT theory to metal insulator metal (MIM) diodes, which have been investigated for solar rectennas,<sup>7–11</sup> but the same approach can be applied to other diodes operating at optical frequencies.<sup>12</sup>

The theoretical efficiency of microwave rectennas used in harvesting narrow and broadband radiation can be high. At such low frequencies and high input intensities the device operating voltage is much larger than  $\hbar\omega/q$ , and the behavior may be treated classically.<sup>13</sup> However, at the low intensities of solar radiation and large  $\hbar\omega/q$ , comparable to the onset of significant nonlinearity in the diode direct current (dc)  $I(V)$  characteristics, nonlinear effects lead to a significant change in the physics used to describe device operation. We address here how this limits the broadband efficiency.

Considering the theoretical efficiency as the dc power produced as a function of alternating current (ac) electrical power dissipated by the diode<sup>14</sup> results in misleadingly high efficiency values. Instead, we consider the efficiency as a function of the radiant power incident at the antenna, which

includes coupling losses from the antenna to the diode. We choose diode characteristics that provide ideal load matching, which limits the diode rectification characteristics but avoids the much larger losses due to poor power coupling.

To calculate efficiency under broadband illumination, we select the power equivalent to one sun incident on the earth's surface (i.e., 1000 W/m<sup>2</sup>). If the current collected by each diode includes components that are out of phase with each other, cancellation and power loss results. Therefore the maximum power supplied to each diode is limited by the area over which the solar radiation is coherent. The coherence efficiency is defined as the coherent power intercepted by the antenna relative to the total incident power.<sup>12,15</sup> For a coherence efficiency of 90% this area corresponds to a radius of  $\sim 19 \mu\text{m}$ . The maximum power coupled to the antenna is then calculated to be approximately  $1.1 \times 10^{-6} \text{ W}$ . We consider the ideal case where the capacitance of the diode is sufficiently small so that there is no resistance-capacitance (RC) falloff at the optical frequencies of interest. We assume a perfect antenna and do not include antenna efficiency limits, which are analyzed elsewhere.<sup>16</sup>

We begin with the Tien-Gordon theory of PAT.<sup>3</sup> Microwave radiation gives rise to a dc tunneling current that occurs in voltage steps of  $\hbar\omega/q$ ,<sup>4</sup> producing an increase in the tunneling current at voltages below the knee of the dark  $I(V)$  curve. This is equivalent to sampling the dc  $I(V)$  curve at voltage steps of  $\hbar\omega/q$ .<sup>3</sup> Mathematically, the above statement is written as

$$I_{\text{illum}} = \sum_{n=-\infty}^{\infty} J_n^2 \left( \frac{qV_{\omega}}{\hbar\omega} \right) \times I_{\text{dark}} \left( V_D + n \frac{\hbar\omega}{q} \right), \quad (1)$$

where  $I_{\text{illum}}$  is the illuminated dc current with photon energy  $\hbar\omega$ ,  $V_{\omega}$  is the amplitude of the ac voltage across the diode,  $V_D$  is the dc operating voltage,  $I_{\text{dark}}$  is the diode dc dark current, and  $J_n$  corresponds to the Bessel function of order  $n$ . At low intensities and high frequencies corresponding to solar radiation, the Bessel terms are significant only for  $n = -1, 0$ , and  $1$ , because the argument  $qV_{\omega}/\hbar\omega$  is small.

<sup>a)</sup> Author to whom correspondence should be addressed. Electronic mail: [moddel@colorado.edu](mailto:moddel@colorado.edu).

The interpretation is that electrons are available for tunneling across the barrier at energies of one photon energy higher and lower than the Fermi level and the initial state itself. The occupation of these states is governed by the corresponding Bessel terms, which are a function of the source intensity and the photon energy.

We illustrate the rectification process in Figs. 1(a) and 1(b) for a diode with piecewise-linear characteristics and negligible reverse leakage currents. In a rectenna diode having a sufficiently low positive turn-on voltage, there is an increase of the tunneling current in the second quadrant of the  $I(V)$  characteristics, providing rectification and power generation. The rectenna circuit consists of antenna voltage source  $\bar{V}_S$  and antenna impedance  $R_S$ . The capacitor  $C$  models the fact that the antenna blocks dc current. We also assume the presence of a large inductor  $L$ , which blocks the ac power from reaching the load  $R_L$  (for optical frequencies the leads to the load serve this function). In this clamping circuit the voltage across the diode consists of the dc self-bias  $V_D$  across the load and an ac voltage  $\bar{V}_\omega$ . The bar over a variable denotes that it is a vector consisting of multiple frequency components.

To determine the antenna source voltage at an incident power  $P_{in}$ , we use a load resistor perfectly matched to the antenna impedance  $R_S$ , which gives  $V_S = \sqrt{8P_{in}R_S}$ . The current through the diode in a rectenna circuit, at a particular dc operating voltage, is calculated as follows. The time domain alternating voltage is treated as a perturbation of the initial electronic states in the diode to determine a phase factor. Diode dark  $I(V)$  characteristics and the phase factor are used to calculate the time-domain rectified current, using the form given by Werthamer<sup>17</sup> and generalized by Tucker.<sup>6</sup> The expression for the average time dependent current  $\langle I(t) \rangle$  is then simplified to

$$\langle I(t) \rangle = \iint d\omega' W(\omega') I_{dark} \left( \omega' + \frac{qV_D}{\hbar} \right) e^{-i\omega't} \times d\omega'' W^*(\omega'') e^{i\omega''t}. \quad (2)$$

Here  $W$  is the phase factor described in Ref. 6 and is the result of modulation of the Fermi level due to an applied ac perturbation,  $I_{dark}$  refers to the diode dark  $I(V)$  characteristics modified by the incoming photon frequency  $\omega$ . For each  $V_D$  the expression is integrated over the range of incident frequencies to calculate the resulting illuminated diode current. Along with the modulated dc current, there are ac currents flowing through the diode at the fundamental input frequency and its harmonics.<sup>6</sup> This requires a harmonic balance approach to determine the voltage across the diode in the presence of circuit impedance. Equation (3) is used to determine the voltage across the diode. The alternating voltage across the diode<sup>18</sup> is

$$\bar{V}_\omega = \bar{V}_S - \bar{I}_\omega R_S. \quad (3)$$

Since  $\bar{I}_\omega$  is itself a function of  $\bar{V}_\omega$ , the equation has to be solved self consistently to reach a stable solution. We iteratively solve for the diode voltage and current to reach steady state values. The rectified dc output power is the product of  $I_{illum}$  and  $V_D$ . Rectenna efficiency is calculated as the ratio of the output dc power to the input ac power. At low  $V_S$  corresponding to solar terrestrial intensities, the harmonics are insignificant compared to the fundamental, but they become significant at high input voltages. The antenna impedance is assumed to be  $100 \Omega$  and independent of frequency.

It can be inferred from Fig. 1(b) that a high reverse resistance is required to minimize the leakage currents and increase the power output in the second quadrant. We

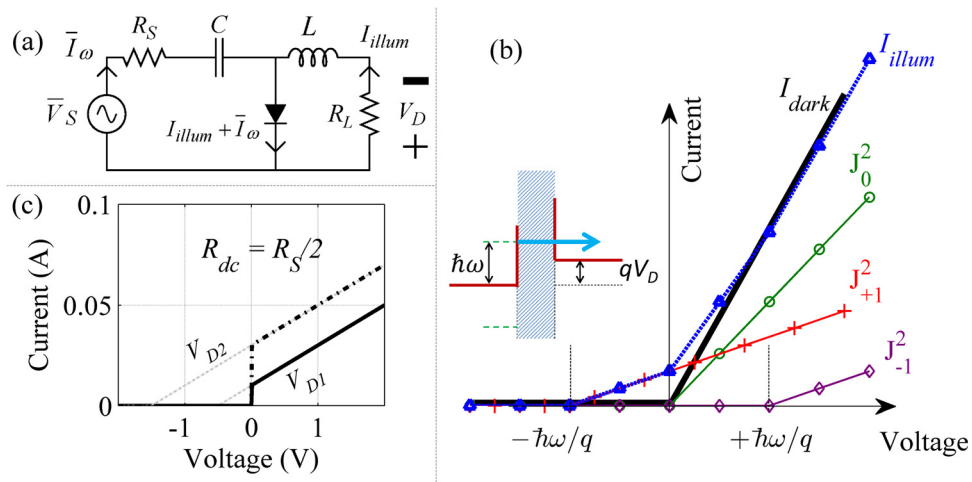


FIG. 1. (a) Rectenna equivalent circuit including a high frequency antenna voltage source  $V_S$  with internal impedance  $R_S$ , and current  $\bar{I}_\omega$ . The voltage across the diode consists of the dc operating voltage  $V_D$  and an ac voltage  $\bar{V}_\omega$ . The inductor  $L$  is large and blocks the ac power from being dissipated in the load. Current through the diode is a combination of the rectified dc current  $I_{illum}$ , the ac fundamental from the antenna, and harmonics produced in the diode. (b)  $I(V)$  characteristics showing the effect of PAT under illumination. The dark  $I(V)$  characteristics are represented by the black solid line. Tunneling currents are produced by photon absorption (red pluses) and emission (purple diamonds), for a photon energy of  $\hbar\omega$ . The combination of these currents produces the dc tunneling current (blue triangles). The inset illustrates the energy band diagram of a typical MIM diode under dc bias. (c) Diode  $I(V)$  characteristics for optimal matching to an antenna, shown at two different rectenna operating voltages:  $V_{D1} = -0.5$  V (solid black) and  $V_{D2} = -1.5$  V (dash-dot black). In the following development of the response as a function of  $V_D$  a diode  $I(V)$  with a different intercept is used for each value of  $V_D$ . The x-axis intercept is the corresponding operating voltage  $V_D$ , and the reciprocal of the slope of the  $I(V)$  (i.e.,  $R_{dc}$ ) is set to half the antenna impedance ( $R_S$ ). This provides an optical frequency secant

assume a diode that has negligible reverse leakage. The presence of source resistance requires impedance matching with the diode for maximum power transfer. The impedance offered by the diode to an input at a particular photon energy is the reciprocal of the slope of a secant between two points on the  $I(V)$  curve, one photon energy above and below the  $V_D$ .<sup>19</sup> This impedance  $R_\omega$  is

$$R_\omega = \frac{2 \times (\hbar\omega/q)}{I_{\text{dark}}(V_D + \hbar\omega/q) - I_{\text{dark}}(V_D - \hbar\omega/q)} \\ \approx \frac{2 \times (\hbar\omega/q)}{I_{\text{dark}}(V_D + \hbar\omega/q)} = \frac{2 \times (\hbar\omega/q)}{m \times (-|V_D| + \hbar\omega/q) + b}. \quad (4)$$

For  $m = 1/R_{dc}$  and  $b = |V_D|/R_{dc}$ , we obtain  $R_\omega = 2R_{dc}$ .

This shows that the impedance offered by the diode to a photon is twice the reciprocal of the slope of a particularly designed dark  $I(V)$  characteristics. We have constructed an  $I(V)$  characteristic to perfectly match the antenna and the diode at a particular  $V_D$  such that its first quadrant differential resistance  $R_{dc}$  is half the antenna impedance and an extrapolation of the  $I(V)$  intercepts on the x-axis at  $V_D$ , as shown in Fig. 1(c). At a particular  $V_D$  the diode impedance is constant and equal for all photon energies  $\hbar\omega$  greater than  $|qV_D|$ . For each value of  $V_D$  a diode having a different  $I(V)$  intercept is required. This is not a realistic resistance characteristic but instead is used to find the maximum theoretical efficiency that can be obtained.

For monochromatic illumination of the rectenna, since there is optimal power transfer all incident power is coupled to the diode. In the quantum limit, there is one electron per incident photon, i.e., unity quantum efficiency.<sup>6</sup> Our simulation produced this current maximum at  $|qV_D| = \hbar\omega$ , as shown in Fig. 2(a), giving a power conversion efficiency of 100%. The current drops to zero when the voltage exceeds this because the PAT no longer provides sufficient energy to surmount the operating voltage barrier required to achieve forward current, as can be seen from the inset in Fig. 1(b). This voltage barrier blocks rectification of photons having  $\hbar\omega < |qV_D|$  just as sub-bandgap energy photons do not contribute to the photocurrent in conventional semiconductor solar cells.

This result shows that for a carefully engineered diode a rectenna operating under monochromatic illumination approaches unity power conversion efficiency. As with conventional solar cells, obtaining close unity efficiency with a realistic  $I(V)$  characteristic would require infinite intensity and well collimated incident radiation,<sup>20</sup> but such an analysis is beyond the scope of this letter. Our result for monochromatic illumination opens the way for applications in room-temperature terahertz sensing and detection, and high frequency power transfer and conversion applications.

At high input intensities or low frequencies, multiple steps appear in the  $I(V)$  due to higher order and mixed excitations. As the intensity increases or the frequency decreases further the results approach the classical expression for large signal rectification,<sup>21</sup> in agreement with the correspondence principle. However, at low intensity and high frequency limits the quantum approach of PAT is required.

To understand the rectification process for the solar spectrum we first consider the case of illumination at two different frequencies  $\omega_1$  and  $\omega_2$ . The distribution of electrons is

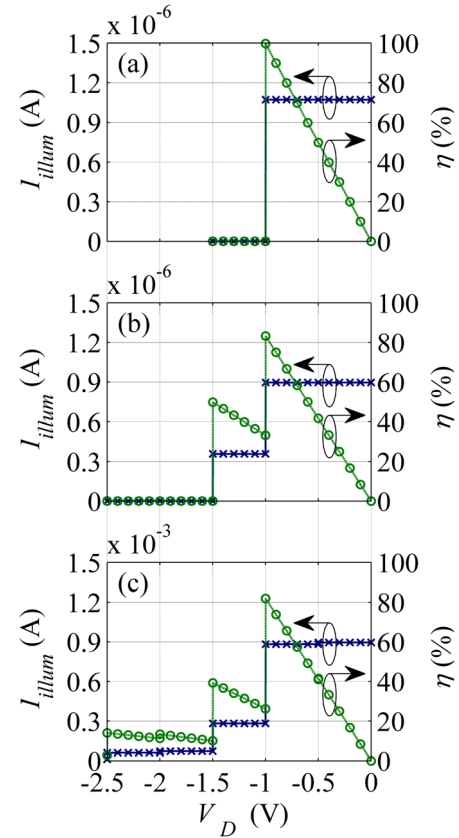


FIG. 2. Illuminated  $I(V)$  (blue crosses) and efficiency  $\eta$  (green circles) characteristics of the diode. (a) Monochromatic illumination. The incident photon energy is 1 eV, and the input power is  $1.1 \times 10^{-6}$  W, corresponding to a solar power of  $1000 \text{ W/m}^2$  over an area with a radius of  $\sim 19 \mu\text{m}$ . Rectenna efficiency approaches 100% when  $|qV_D|$  approaches  $\hbar\omega$ . (b) Two frequency illumination corresponding to photon energies of 1 eV and 1.5 eV for the same total input power. The voltage amplitude of the two sources is equal and the fraction of the number of low to high energy photons is 1.5:1. (c) Same as (b), with increased input power corresponding to  $10^3$  suns, showing the appearance of tunneling current at high reverse operating voltages due to excitation of both higher order and mixing terms.

still discrete but gives rise to states at energies  $\hbar\omega_1/q$  and  $\hbar\omega_2/q$ , and sum and difference energies  $\hbar(\omega_1 + \omega_2)/q$  and  $\hbar(\omega_1 - \omega_2)/q$  due to mixing. As with the higher order terms in the monochromatic case, higher order mixing occurs at high input intensities and low input frequencies, giving rise to multiple sum and difference combinations of the two. The time-dependent voltage across the barrier in the simplest case of two-frequency illumination is given as

$$V(t) = V_D + V_1 \cos(\omega_1 t) + V_2 \cos(\omega_2 t) \quad (5)$$

In Eq. (5),  $V_1$  and  $V_2$  are the voltage amplitudes across the diode at the two frequencies  $\omega_1$  and  $\omega_2$ . We derive the expression for the illuminated dc current following Tucker's approach

$$I_{\text{illum}} = \sum_{m=-\infty}^{\infty} \sum_{n=-\infty}^{\infty} J_m^2 \left( \frac{qV_1}{\hbar\omega_1} \right) J_n^2 \left( \frac{qV_2}{\hbar\omega_2} \right) \\ \times I_{\text{dark}} \left( V_D + m \frac{\hbar\omega_1}{q} + n \frac{\hbar\omega_2}{q} \right). \quad (6)$$

In Eq. (6),  $m$  and  $n$  are the photon absorption or emission numbers for the two different frequencies.

The simulated  $I(V)$  characteristic for illumination at two frequencies, corresponding to photon energies of 1 eV and 1.5 eV, is shown in Fig. 2(b). The calculations were performed using a harmonic balance analysis method where multiple harmonics of the incident frequencies and the mixed frequencies were included. Steps appear at  $|qV_D|$  equal to the photon energies. The efficiency is lower than for the single frequency case because for smaller magnitude operating voltages the full photon energy of the higher energy photons is not used, and at larger magnitude operating voltages the lower energy photons do not contribute to the current.

A way to increase the efficiency is to channel the unused photons to higher energy states through higher order and mixing terms in Eq. (6), which would give rise to non-zero current at operating voltages of less than  $-1.5$  V. As seen in Fig. 2(b) neither of these processes contribute significantly to the current-voltage characteristics at solar intensities because the occupation probabilities of the higher order and mixed states, as represented by the higher order Bessel terms in Eq. (6), are significantly lower than the fundamental states. At high intensities photon stepping at these higher order and mixed energies is observed, as shown in Fig. 2(c). In reality, however, rectennas cannot make use of a concentrated sunlight because of the coherence limitation described earlier. Improving the  $I(V)$  characteristics would also increase the strength of the mixed states, but at the cost of a poorer impedance match with the antenna.

To analyze solar conversion efficiency we model the solar spectrum as a blackbody at 5780 K and consider the maximum terrestrial input power ( $P_{in}$ ) of  $1.1 \times 10^{-6}$  W. This determines the shape of the solar intensity spectrum. The shape of the source voltage spectrum ( $\bar{V}_S$ ) is given by the square root of the solar intensity spectrum. We assume a constant antenna impedance of  $100 \Omega$  using the constructed  $I(V)$  characteristic of Fig. 1(c). The source voltage amplitude is set such that the power dissipated in a matched load resistor is the same as the coherent power from the sun captured by the antenna ( $P_{in}$ ). To determine the time-dependent voltage waveform and the phase factor we take the inverse Fourier transform of this source voltage spectrum. Then we use Eqs. (2) and (3) simultaneously to obtain the illuminated current under multispectral illumination and the diode alternating voltage ( $\bar{V}_\omega$ ), as shown in Fig. 3.

The maximum efficiency of  $\sim 44\%$  is produced at an operating voltage of 1.1 V. This result is reminiscent of the Trivich-Flinn efficiency of solar energy conversion by quantum processes,<sup>22,23</sup> also proposed later as the Shockley-Queisser ultimate efficiency for devices having bandgap cut-off. The Trivich-Flinn efficiency provides the efficiency of devices with a bandgap that absorb only energy above the threshold. With rectenna solar cells, operating voltage  $|qV_D|$  plays the role that bandgap plays in conventional solar cells, so that only photons having an energy equal to  $|qV_D|$  are used optimally. Lower energy photons are wasted and the energy of higher energy photons is only partially used. Under the conditions employed here, we obtain virtually no advantage from mixing and higher order terms, due to the low input intensity. This maximum efficiency is higher than the Shockley-Queisser<sup>2</sup> limit of 33%, which is reduced from 44% due to the finite temperature of the cell and radiative

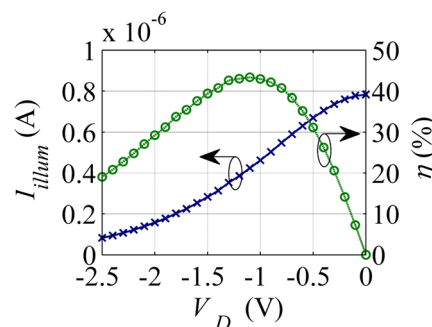


FIG. 3.  $I(V)$  (blue crosses) and efficiency (green circles) characteristics of the diode for an ideal rectenna under solar blackbody illumination at 5780 K. The input power is  $1.1 \times 10^{-6}$  W. This is the maximum power available due to coherence issues. The diode dark  $I(V)$  characteristics have a shape like that shown in Fig. 1(c), but with a slope and intercept designed for optimal power coupling from the antenna for each operating voltage. The maximum efficiency is  $\sim 44\%$ .

recombination in the diode. In this letter, we have not included these effects, which require device thermodynamic analysis,<sup>24</sup> nor limits imposed by the antennas. As with multi-gap conventional solar cells, the conversion efficiency of rectenna solar cells can be increased with the use of spectral splitting and rectenna solar cells at different operating voltages. Because spectral splitting with rectennas does not require materials matched to each spectral range, rectenna solar cells have an inherent advantage in this process.

The maximum conversion efficiency we found is limited because there are no mixing or higher order terms at solar terrestrial intensity. In contrast, microwave rectennas make use of substantial mixing of low energy photons at high operating voltage, and attain higher conversion efficiencies.

Although the optical rectenna results were developed here for the case of metal-insulator-metal diodes, the same semi-classical characteristics are expected for other diode types operating at optical frequencies.<sup>12</sup>

In this letter we explored the efficiency limits of rectenna solar cells. We developed the calculations based on the theory of PAT and showed that, for diodes that are optimally matched to antennas, monochromatic power conversion efficiencies approach 100% and the multispectral efficiency is limited to 44% at solar terrestrial intensities. Spectral splitting can improve the efficiency, and can be accomplished simply by setting the operating voltage for each rectenna to rectify the desired spectral range.

The authors gratefully acknowledge S. Grover for helpful discussions. This work was carried out under a contract from Abengoa Solar.

<sup>1</sup>R. L. Bailey, *J. Eng. Power* **94**, 73 (1972).

<sup>2</sup>W. Shockley and H. J. Queisser, *J. Appl. Phys.* **32**, 510 (1961).

<sup>3</sup>P. K. Tien and J. P. Gordon, *Phys. Rev.* **129**, 647 (1963).

<sup>4</sup>A. H. Dayem and R. J. Martin, *Phys. Rev. Lett.* **8**, 246 (1962).

<sup>5</sup>J. Tucker, *IEEE J. Quantum Electron.* **15**, 1234 (1979).

<sup>6</sup>J. R. Tucker and M. J. Feldman, *Rev. Mod. Phys.* **57**, 1055 (1985).

<sup>7</sup>B. J. Eliasson, Ph.D. dissertation, University of Colorado, Boulder, 2001.

<sup>8</sup>B. Berland, Subcontractor Report NREL/SR-520-33263, 2003.

<sup>9</sup>S. Grover and G. Moddel, *Solid-State Electron.* **67**, 94 (2012).

<sup>10</sup>R. Corkish, M. Green, and T. Puzzer, *Sol. Energy* **73**, 395 (2002).

<sup>11</sup>D. Y. Goswami, S. Vijayaraghavan, S. Lu, and G. Tamm, *Sol. Energy* **76**, 33 (2004).

- <sup>12</sup>S. Grover, Ph.D. dissertation, University of Colorado, Boulder, 2011.
- <sup>13</sup>A. Sanchez, C. F. Davis, K. C. Liu, and A. Javan, *J. Appl. Phys.* **49**, 5270 (1978).
- <sup>14</sup>T.-W. Yoo and K. Chang, *IEEE Trans. Microwave Theory Tech.* **40**, 1259 (1992).
- <sup>15</sup>H. Mashaal and J. M. Gordon, *Opt. Lett.* **36**, 900 (2011).
- <sup>16</sup>G. A. E. Vandenbosch and Z. Ma, *Nano Energy* **1**, 494 (2012).
- <sup>17</sup>N. R. Werthamer, *Phys. Rev.* **147**, 255 (1966).
- <sup>18</sup>S. Withington, P. Kittara, and G. Yassin, *J. Appl. Phys.* **93**, 9812 (2003).
- <sup>19</sup>S. Grover, S. Joshi, and G. Moddel, "Theory of operation for rectenna solar cells," *J. Phys. D: Appl. Phys.* **46** (in press); S. Grover and G. Moddel, *IEEE J. Photovoltaics* **1**, 78 (2011).
- <sup>20</sup>M. A. Green, *Prog. Photovoltaics* **9**, 257 (2001).
- <sup>21</sup>C. A. Hamilton and S. Shapiro, *Phys. Rev. B* **2**, 4494 (1970).
- <sup>22</sup>D. Trivich and P. A. Flinn, in *Solar Energy Research*, edited by F. Daniels and J. A. Duffie, 1st ed. (University of Wisconsin Press, 1955), p. 143.
- <sup>23</sup>M. A. Green, *Prog. Photovoltaics* **20**, 127 (2012).
- <sup>24</sup>T. Markvart, *Appl. Phys. Lett.* **91**, 064102 (2007).